Scientific
Research
Publishing

Contribution to the Modeling of a Solar Adsorption Refrigerator under the Climatic Conditions of Burkina Faso

Guy Christian Tubreoumya[1,2,3], Alfa Oumar Dissa[1], Eloi Salmwendé Tiendrebeogo[1], Xavier Chesneau[2], Aboubacar Compaoré[1], Kayaba Haro[1], Charles Didace Konseibo[3], Belkacem Zeghmati[2], Jean Koulidiati[1]

[1]Laboratoire de Physique et de Chimie de l'Environnement (L.P.C.E), Université Ouaga I, Ouagadougou, Burkina Faso
[2]LAboratoire de Mathématiqueset PhySique (LA.M.P.S), Université de Perpignan Via Domitia (UPVD), Perpignan, France
[3]Centre Ecologique Albert Schweitzer (CEAS), Ouagadougou, Burkina Faso
Email: guytubreoumya@yahoo.fr

Abstract

This work concerns a dynamic modeling and a numerical simulation of the operation of an adsorption solar refrigeration system using the zeolite-water couple. For this, a mathematical model representing the evolution of heat and mass transfer at each component of the solar adsorption refrigerator has been developed. We have adopted the Dubinin-Astakhov model for the adsorption kinetics of the zeolite/water pair. This model allows to describe the phenomenon of adsorption and to calculate the rate of adsorbate (water) in the zeolite (adsorbent) as a function of the temperature and the pressure. The equations governing the operation of the solar adsorption refrigerator, deduced from the thermal and mass balances established at the collector adsorber, condenser and evaporator components, were solved by an implicit finite difference scheme and Gauss Seidel's iterative method. We have validated the model established by applying it to the model of Allouhi *et al.* 2014. We analyzed the influence of the adsorbate/adsorbent couples, the solar flux, the ambient temperature on the adsorption and desorption process. The temperature profiles obtained representing the temperature evolution of the glass, the absorbent plate, the zeolite-water mixture, the condenser, the evaporator, as well as the pressure and the adsorbed mass allowed us to evaluate the performance of the solar adsorption refrigerator. SCOP is higher the higher the solar flux captured by the collector-adsorber.

1. Introduction

Cold production is mainly achieved by compression machines whose operation requires the use of refrigerants and excessive consumption of electrical energy. These refrigerants, CFCs (chlorofluorocarbons), HCFCs (hydrochlorofluorocarbons) and HFCs (hydrofluorocarbons) are harmful to the ozone layer and contribute to an increase in the greenhouse effect. Since the Montreal Protocol in 1987, international agreements have been signed to reduce emissions of these refrigerants [1]. Thus, research efforts focused on the development of refrigeration technologies, which respond to environmental and energy concerns, have been undertaken. Solar adsorption refrigeration machines have been the subject of numerous studies [2] [3] [4].

These machines are an alternative to solve both ecological and energy problems. Indeed, the technology of these machines is simple, maintenance is easy, and the materials used, are recyclable [5]. In addition, these machines use refrigerants such as water [6], methanol [7] and ammonia [8], which have no effect on the environment. For countries such as Burkina Faso, with favorable sunshine with an average irradiation between 5.5 kWh·m^{-2}·day^{-1} and 65 kWh·hm^{-2}·day^{-1} [9], solar adsorption refrigeration is a promising solution to meet important needs such as food preservation, pharmaceuticals, air conditioning, etc. and also to reduce electricity consumption.

However, some disadvantages have become obstacles to the actual application and marketing of these machines such as discontinuous cycle operation [10] [11], low coefficient of performance, poor heat and mass transfer in the bed Adsorbent [12], low thermal conductivity of the adsorbent [13] [14] [15], poor contact between the surface of the adsorber and the adsorbent [16] [17].

To improve the performance of solar adsorption refrigeration machines, numerous research axes have been proposed, studied and tested. Thus, several solar collector models have been used by researchers to optimize the solar radiation received through use: vacuum tube collectors [18] [19] [20] of the single-glazed or double-glazed (TIM) flat plate collectors [21] [22] [23], cylindro-parabolic collectors [24] [25].

Other approaches based on the shape of the adsorber have been used to improve the efficiency of solar radiation. Thus, flat, tubular adsorbers, equipped with external or internal fins, have been used in several prototypes of adsorption solar refrigerators. These fins act as thermal bridges between the absorbent plate and the reactive (porous) medium and thus optimize the heat and mass transfer in the adsorbent bed [12] [17] [26] [27] [28].

In addition, some researchers have focused on improving the thermal conductivity of adsorbents through the development of composite adsorbent. The technique for preparing the consolidated composite adsorbents consists in adding a material having a higher thermal conductivity to the powder of the conventional solid adsorbent. By this technique, thermal conductivity of the order of 5 to 15 W/m·k can sometimes be reached and a heat exchange coefficient with the metal walls of the adsorber ranging from 200 to 3000 W/m^2·k [26] [29] [30]

[31] [32] [33].

In addition, to overcome the intermittent character of the solar adsorption refrigeration cycle, prototype models of machines have been developed. These machines consist of two beds of adsorbents operating so that one adsorbs the refrigerant and the other one desorbs it. Thus, they make it possible to produce cold continuously [7] [34] [35] [36].

The efficiency of the operation of the refrigerating machines is also linked to the climatic conditions of the site in which the machine is located. Thus, several experimental studies on prototypes of adsorption solar refrigerators have been proposed and tested, in order to find their actual behavior [23] [37] [38] [39] [40].

The main objective of this study is to contribute to the understanding of the solar refrigeration system by adsorption through a dynamic modeling of a solar adsorption refrigerator model operating under the climatic conditions of Burkina Faso.

2. Materials and Methods

2.1. Description of the Cycle of Operation of the Solar Adsorption Refrigerator

A solar refrigerating adsorption machine operates in a cycle. It consists in a flat plate collector containing the zeolite/water mixture and plays a role of capturing and releasing the heat. It is connected to a condenser and an evaporator. The principle of operation of these machines is based on the phenomena of adsorption-desorption of a gas (water vapor) in a solid (zeolite). This chemical reaction is exo or endothermic according to its direction of unwinding. This ideal cycle represents the evolution of the state of the adsorbent/adsorbate mixture contained in the collector-adsorber. Each cycle includes two main stages governing the operation: one stage for heating the zeolite/water mixture and another for cooling the same mixture.

2.1.1. Heating Phase
- Isosteric heating phase (1 → 2)

At the beginning of the cycle (point 1), the zeolite/water mixture is at its minimum temperature T_a (adsorption temperature) and at the pressure P_{ev} (evaporation pressure); at this time, the collector-adsorber is isolated. Under heating, the pressure and temperature of the mixture increase, while the total mass of adsorbed water remains constant along the transformation (1 → 2) and equal to q_{max}. This pressurization phase ends as soon as the pressure becomes equal to that prevailing in the condenser P_{cd} (point 2). The temperature reached is called desorption threshold temperature T_{s1}.
- Condensation desorption phase (2 → 3)

This phase begins when the pressure of the mixture in the adsorber reaches the condensation pressure P_{cd} (saturation pressure corresponding to the temperature of the condenser), the adsorber is placed in communication with the

condenser and the desorption of the refrigerant begins, which condenses in the condenser thereafter. The adsorber is then in high pressure and follows the iso-bar imposed by the condenser. While continuing heating, the temperature of the mixture in the adsorber increases to the maximum temperature T_g (regenera-tion temperature) at point 3, set for the corresponding cycle. This phase is gen-erally called generation because it is that which makes the adsorber conducive to a new phase of refrigeration production.

2.1.2. Cooling Phase

- Isosteric cooling phase (3 → 4)

In contrast to the first phase, cooling of the zeolite/water mixture begins at point 3, where the temperature and pressure decrease until the pressure becomes equal to that in the evaporator. The temperature reached is referred to as the adsorption threshold temperature T_{s2} (point 4). The total mass of the adsorbed fluid remains constant during this phase and is equal to q_{min}.

- Adsorption-evaporation phase (4 → 1),

This phase is the motor phase of the cycle during which the cold is produced. At point 4, the evaporation of the refrigerant begins, producing cold in the eva-porator. The vapor produced is adsorbed again in the adsorber until the temper-ature of the zeolite water mixture becomes minimal T_a, set for the correspond-ing cycle. During the transformation (4 → 1), the system follows the isobara im-posed by the evaporator and which corresponds to the saturation pressure of the refrigerant (water) at the evaporation temperature. At this point, the machine is ready for a new cycle.

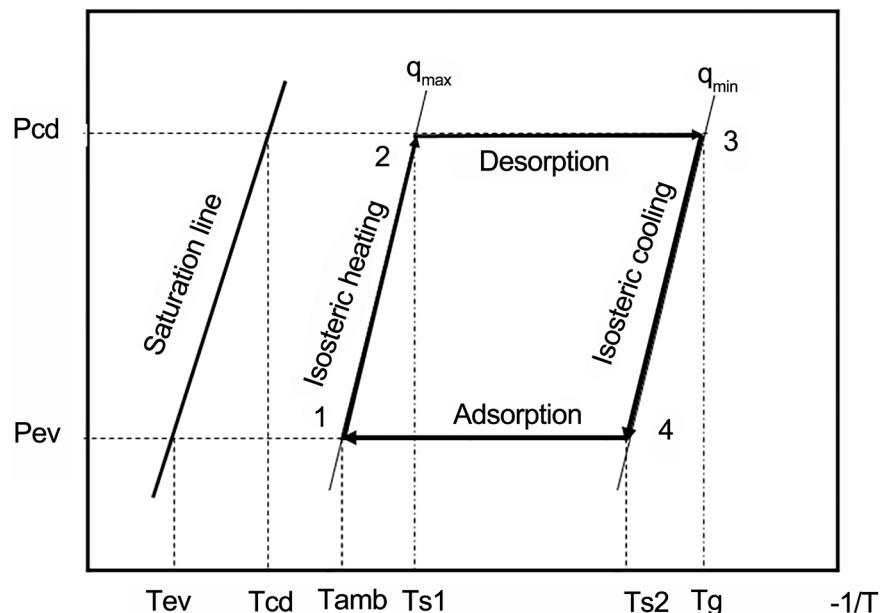Figure 1 shows the basic thermodynamic route of such a machine in the Cla-peyron diagram (LnP; -1/T) (Figure 2).

Figure 1. Theoretical cycle of an adsorption machine.

Figure 2. Photography of solar adsorption refrigerator.

2.2. Modelisation

The mathematical model presented below simulates the real operation of the solar adsorption refrigeration system taking into account the variation in solar radiation and the ambient temperature during the day. Thus, we present the modeling of the transfer of heat and mass in the adsorbent bed, and the balance equations at each compartment of the system (glass, absorbent plate, condenser, and evaporator).

2.2.1. Assumptions

The formulation of some assumptions is necessary for an approximate simulation of the system. Thus we assume that:

- The porous material (adsorbent) is assimilated to a medium having a temperature T and equivalent thermal conductivity,
- Heat transfer is unidirectional,
- The convective heat transfer and the pressure losses are neglected in the porous medium,
- The pressure remains constant in the condenser and in the evaporator.

2.2.2. Equations Balances

The heat transfer equations at each part of the refrigerator can be written as follows:

The glass

$$m_v C_{pv} \frac{dT_v}{dt} = \alpha_v \cdot G_n \cdot s_v + U_{p-v} \cdot s_v \left[T_p - T_v \right] - h_{cv-v-ext} \cdot s_v \left[T_v - T_{amb} \right] \\ - h_{r-v-ciel} \cdot s_v \left[T_v - T_{ciel} \right] \tag{1}$$

The absorbent plat

$$m_p C_{p_p} \frac{dT_p}{dt} = \alpha_p \lambda_v \cdot s_p \cdot G_n - U_{p-v} \cdot s_v \left(T_p - T_v \right) - U_{p-ads} \cdot s_p \left(T_p - T_{zeo} \right) \tag{2}$$

The adsorbent bed

During the isoteric heating and desorption phase

$$m_{eq}c_{peq}\frac{dT_{zeo}}{dt}=U_{p-ads}\cdot s_{p}\left(T_{p}-T_{zeo}\right)$$
$$+\delta\left(\Delta H_{des}m_{ads}\frac{dq^{d}}{dt}+m_{ads}c_{pl}\left(T_{zeo}-T_{cd}\right)\frac{dq^{d}}{dt}\right) \quad (3)$$

During the isoteric cooling phase and adsorption

$$m_{eq}c_{peq}\frac{dT_{zeo}}{dt}=U_{p-ads}\cdot s_{p}\left(T_{p}-T_{zeo}\right)$$
$$+\delta\left(\Delta H_{ads}m_{ads}\frac{dq^{a}}{dt}-m_{ads}c_{pl}\left(T_{zeo}-T_{ev}\right)\frac{dq^{a}}{dt}\right) \quad (4)$$

With:

$\delta=0$: During isoteric heating and cooling;

$\delta=1$: During desorption and adsorption;

The condenser

$$\left[m_{cd}\cdot c_{pcd}+M_{d}\left(t\right)\cdot c_{pl}\right]\frac{dT_{cd}}{dt}$$
$$=m_{ads}\cdot\frac{dq^{d}}{dt}\left(L_{cd}\left(T_{cd}\right)+c_{pl}\left(T_{eau}-T_{cd}\right)\right) \quad (5)$$
$$-h_{r-cd-ciel}\cdot S_{cd}\left(T_{cd}-T_{ciel}\right)-h_{cv-cd-amb}\cdot S_{cd}\left(T_{cd}-T_{amb}\right)$$

The evaporator

$$\left[m_{ev}c_{pev}+\left(M_{d}\left(t\right)-\Delta q.m_{ads}\right)c_{pl}\right]\frac{dT_{ev}}{dt}$$
$$=-m_{ads}\frac{dq}{dt}\left[L_{ev}\left(T_{ev}\right)+c_{pl}\left(T_{eau}-T_{ev}\right)\right]-h_{cv-ev-air}S_{ev}\left(T_{ev}-T_{air}\right) \quad (6)$$

2.2.3. Model of Adsorption Kinetics

Several theories of adsorption have been proposed in the literature to describe the process of the adsorption and desorption phenomenon. The Dubinin-Astakhov equation is used successfully to describe the adsorption of gas vapor on the adsorbent. Thus, this equation is used to calculate the rate of adsorbate (water) in the zeolite (adsorbent) as a function of temperature and pressure.

$$q=w_{0}\rho_{l}\left(T\right)\exp\left(-D\left(T\ln\frac{P_{s}\left(T\right)}{P}\right)^{n}\right) \quad (7)$$

where $\rho_{l}\left(T\right)$ is the density of the adsorbate (water) and $P_{s}\left(T\right)$ is the saturation pressure. w_{0} is the maximum adsorption capacity; D and n are constants pedending on the adsorbent/adsorbate couple used.

2.2.4. System Performance

The solar performance coefficient (SCOP) of a solar refrigerating machine is defined as the ratio between the amount of cold produced at the evaporator and the total solar energy incident for a full day.

$$SCOP=\frac{Q_{f}}{\int_{t_{sr}}^{t_{ss}}A_{s}.G_{n}.dt} \quad (8)$$

where As is the collecting surface and Gn is the solar flux in W/m² Q_f is the amount of cold produced at the evaporator, given by:

$$Q_f = m_{ads} \Delta m \left[L(T_{ev}) - \int_{T_{ev}}^{T_{cd}} Cp_l(T) dT \right] \tag{9}$$

2.3. Numerical Methodology

2.3.1. Initial and Boundary Conditions

For all $t \prec t_0$, t_0 being the instant from which the collector-adsorber is subjected to the solar flux, we have:

$$T_v(t_0) = T_p(t_0) = T_{ev}(t_0) = T_{cd}(t_0) = T(t_0) = T_{amb} \tag{10}$$

$$P(t_0) = P_{ev} = P_s(T_{ev}) \tag{11}$$

$$q = q(T_{amb}, P_{ev}) \tag{12}$$

2.3.2. Method of Resolution

The method of solving the system of equations which describes the transient behavior of the model is purely numerical and based on the implicit finite difference method and the Gauss Seidel iterative method. We have developed and written in Fortran a computer program to model and simulate the adsorption-desorption kinetics of the zeolite/water pair and on the other hand the operation of each element of the refrigerator during a day.

3. Results and Discussion

3.1. Validation of the Model

In order to validate our numerical code, we applied our code to the solar adsorption refrigerator model presented by A. Allouhi *et al.* [41]. This model describes a parallelepiped-shaped collector-adsorber refrigerator using the silicagel-water couple. A comparison between the changes in the temperature in the adsorbent bed as a function of its pressure, describing the Clapeyron cycle of the solar adsorption refrigerator, shows good quantitative agreement. Indeed, the maximum deviation observed for the temperatures is of the order of 1.1% and 2.4% for the pressure (**Figure 3**).

3.2. Climatic Data

Solar radiation and ambient temperature are parameters that affect the performance of solar refrigeration systems. Thus, using the weather data provided by the General Direction of Meteorology in Burkina Faso (DGM), which include the values of the monthly global radiation densities on a horizontal plane in J/cm², we used the method of Liu and Jordan to transform these data in order to obtain the hourly values of the global radiation on an inclined plane of angle 12.2° with respect to the horizontal. For ambient temperature, we used the data of E. Ouédraogo *et al.* [42], who carried out a statistical study to develop an hourly weather file for the city of Ouagadougou. Thus, **Figure 4(a)** and **Figure 4(b)**
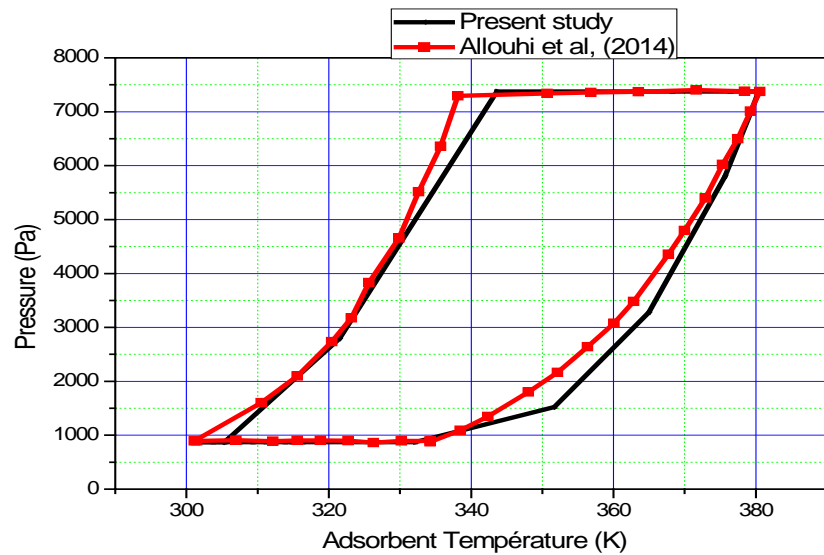
Figure 3. Comparison of the Clapeyron cycle given by A. Allouhi and our calculation code.

Table 1. Main parameters used in the simulation.

Symbols	Paramters	Values	Units
Properties of the adsorbent/adsorbate (zeolite/water)			
Cp_{ads}	Chaleur spécifique	0.836	$[kJ \cdot kg^{-1} \cdot K^{-1}]$
m_{ads}	Masse	32	$[kg]$
ρ_{ads}	Densité	620	$[kg \cdot m^{-2}]$
Cp_l	Chaleur spécifique	4.18	$[kJ \cdot kg^{-1} \cdot K^{-1}]$
Collector-adsorber			
ε_v	Emissivity of the glass	0.9	[-]
τ_v	Transmitivity of the glass	0.95	[-]
α_v	Absorptivity of the glass	0.05	[-]
e_v	Thickness of the glass	0.04	$[m]$
S	Area	1	$[m^2]$
Cp_v	Specific heat of the glass	0.75	$[kJ \cdot kg^{-1} \cdot K^{-1}]$
Cp_p	Specific heat of the absorbent plate	0.896	$[kJ \cdot kg^{-1} \cdot K^{-1}]$
e_p	Thickness of absorbent plate	0.05	$[m]$
α_p	Absorptivity of absorbent plate	0.95	[-]
ε_p	Emissivity of the absorbent plate	0.9	[-]
Parameters of Dubinin-Astakhov			
D	Characteristic parameter of the adsorbent/adsorbate couple	$4.15 \ 10^{-7}$	[-]
n	Characteristic parameter of the adsorbent/adsorbate couple	2	[-]
W_o	Maximum adsorption capacity	$0.269 \ 10^{-3}$	$[m^3 \cdot kg^{-1}]$
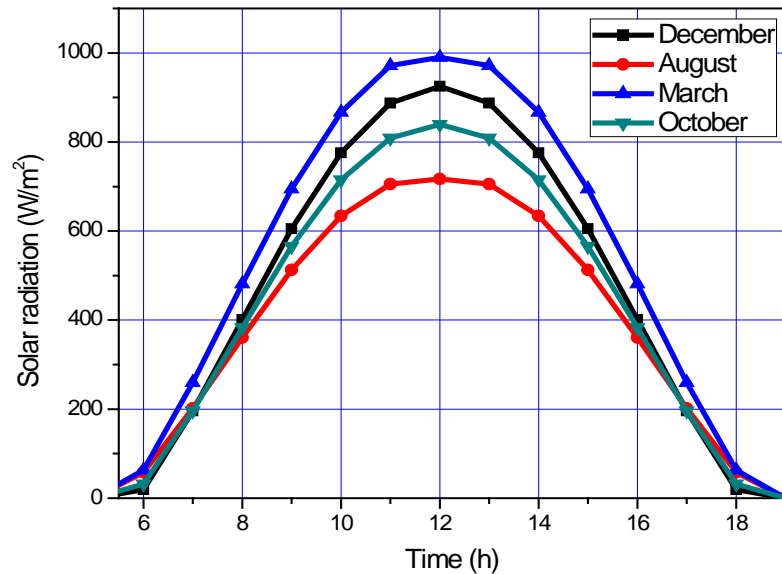
(a)
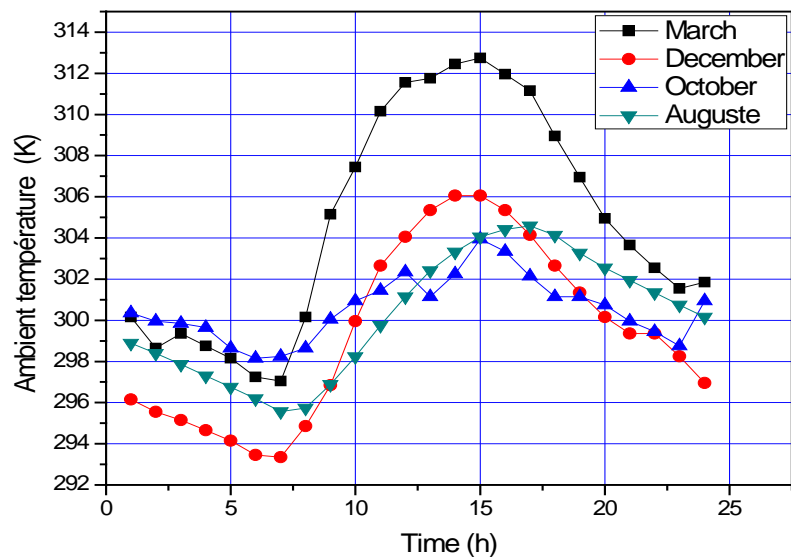
(b)

Figure 4. Hourly evolution of solar radiation and ambient temperature.

shows the hourly evolution of global solar radiation and the ambient temperature for December, August, October and March. It can be seen that the radiation is maximum in March and minimal in August, this can be explained by the clear sky in March and by a sky low in October and December. In August, this is due to the presence of dust and clouds. These values thus obtained and the values in **Table 1** were used for the simulation of our model.

3.3. Dynamic Behavior of the Solar Refrigerator

Figure 5 shows the evolution of the temperature of the glass, the absorbent plate and the adsorbent bed (zeolithe) as a function of time during the four phases of
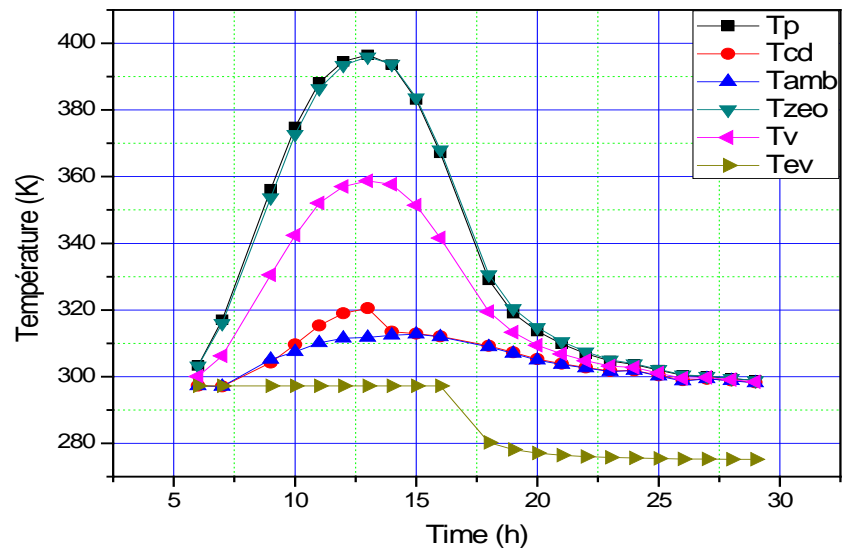
Figure 5. Time evolution of the temperature of the various components of the solar refrigerator for the month of March.

the cycle. At the beginning of the cycle (the initial state), the temperatures are uniform and equal to the adsorption temperature, which in turn equals the ambient temperature at sunrise. When the solar flux increases, the collector-adsorber heats up and the temperatures of its various components increase rapidly with time. They each reach a maximum (Tv = 358 K, Tp = 396 K, Tzeo = 395 K) at about 13 o'clock. The maximum temperature of the adsorbent bed is referred to as the regeneration temperature, that is to say the temperature at which there is no heat exchange between the plate and the adsorbent bed. When the solar flux decreases, the collector-adsorber cooling begins. The temperatures of the various compartments decrease until the temperature reaches 300 K. This temperature represents the temperature in which there is no exchange between the glass pane, the plate and the adsorbent bed.

The evolution of the temperature of the condenser during the cycle is also shown in **Figure 5**. At the beginning of the cycle, the temperature of the condenser is the same as that of the ambient. This is explained by the fact that the condenser is isolated from the collector-adsorber during this period. When the desorption-condensation phase begins, the self-contained valve opens and the desorbed water vapor flows into the condenser, resulting in an increase in its temperature. At about 14 o'clock, the temperature of the condenser reaches its maximum at Tcd = 320 K, after which it begins to decrease. This increase in condenser temperature is due in large part to the latent heat of condensation of the water. The decrease of the temperature after 14 o'clock is due, on the one hand, to the cessation of the desorption process and, on the other hand, to cooling by means of the convection and the radiation which the condenser exchanges with the ambient medium. The temperature of the condenser begins to follow that of the ambient temperature during the rest of the day.

The evolution of the temperature of the evaporator is also shown in the same Figure 5. The temperature of the evaporator decreases from 297 K to 275 K. This cooling of the evaporator is due to the evaporation of the condensate (water) from the evaporator to the adsorbent bed. Thus, the adsorbate withdraws the needed heat for phase change of the refrigerating enclosure where the evaporator is located. This results in cooling.

Figure 6 shows the variation of the pressure within the adsorbent bed as a function of time. During the phases of the operating cycle, the pressure has a logical behavior with the evolution of the temperature. It increases rapidly from the evaporation pressure Pev = 872 Pa (equal to the saturation pressure at the evaporation temperature) up to a maximum value corresponding to the condensation pressure Pcd = 7376 Pa (equal to the saturation pressure at the condensation temperature). During the desorption phase, the pressure remains constant and equal to the condensation pressure until the temperature of the adsorbent bed reaches the maximum regeneration temperature. Then, it begins to decrease to the low initial evaporation pressure.

The distribution of the quantity of water adsorbed during the four phases of the cycle is also shown in the same figure. During the cycle, the total quantity of water adsorbed in the adsorbent bed decreases during the desorption phase and then increases during adsorption. It remains constant during the isosteric heating and cooling phases.

3.4. Comparison of the Results of the 4 Months

The evolution of the temperature, the pressure and the quantity of water adsorbed in the adsorbent bed are respectively represented in Figures 7-9. It is clear that the climatic data have a great influence on the Performance of the solar refrigerator. Indeed, for the month of March, the values of the temperature,
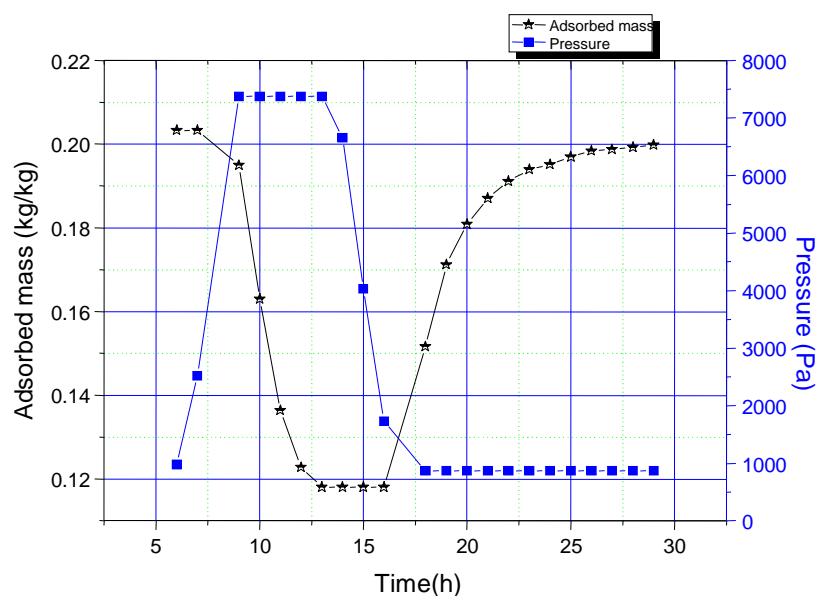

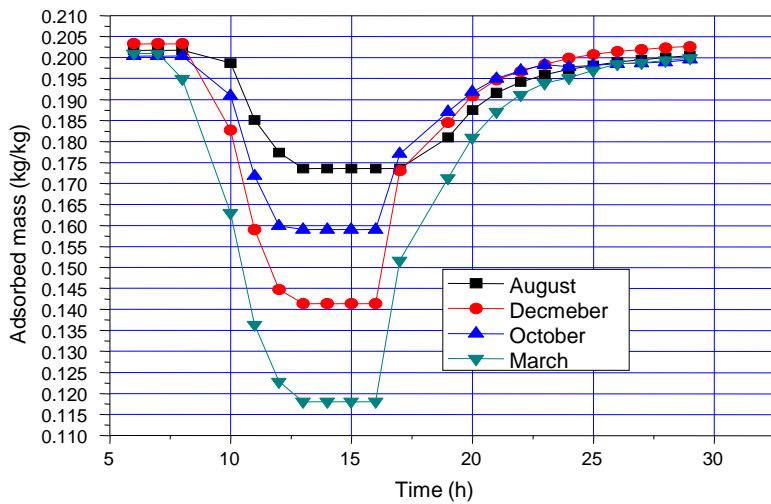**Figure 6.** Evolution of the pressure and the adsorbed mass for the month of March.

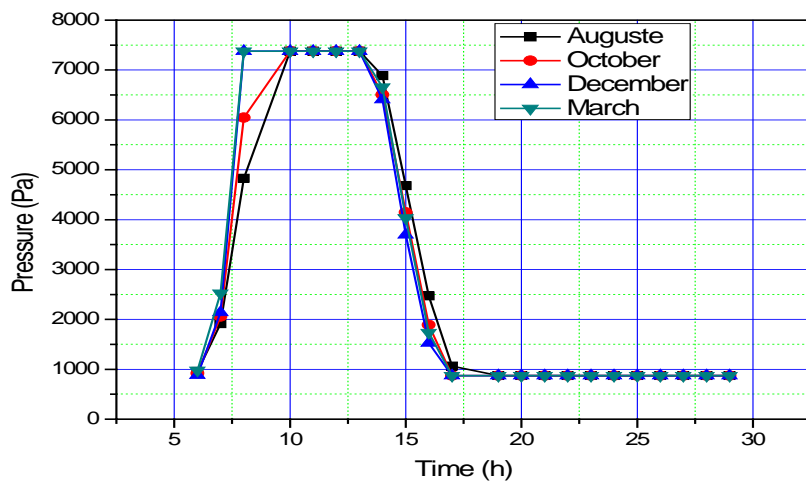**Figure 7.** Comparison of the evolution of the adsorbed mass during the 4 months.

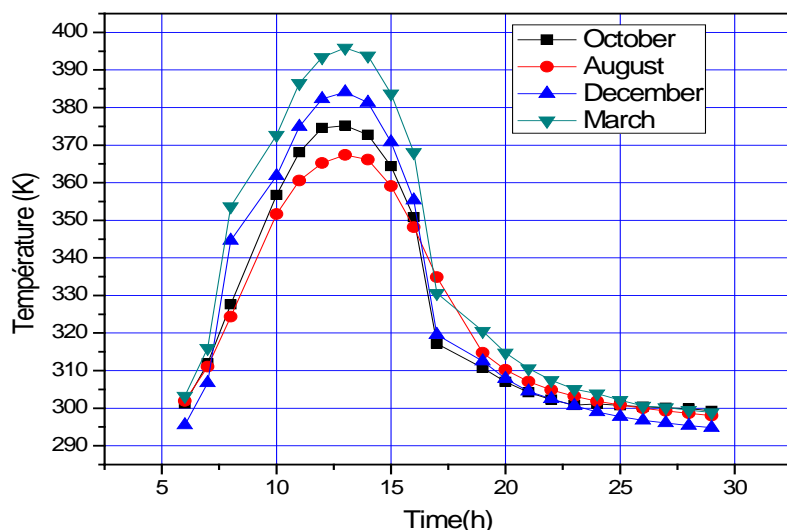**Figure 8.** Comparison of the evolution of the pressure during the 4 months.

Figure 9. Comparison of the evolution of the temperature of the zeolite during the 4 months.

Table 2. Coefficient of performance of the solar adsorption refrigerator.

Month	August	October	December	March
Qf [MJ]	2,1098	3,0965	4,642	6,391
Gn-moy (W/m²)	435,597	479,980	514,916	589,636
SCOP	0,113	0,151	0,211	0,253

of the quantity of desorbed adsorbate, are higher compared to the other three months. This is due to the fact that the solar flux density is maximum during this month (990 W/m^2). The performances of the solar adsorption refrigerator for the four months are also shown in the Table 2. For the month of March, the SCOP reached is 0.25, while for the other months the SCOP is equal to 0.21 for the month of December, 0.15 for the month of October and 0.11 for the month of August.

4. Conclusions

This work presents the modeling of a system of solar refrigeration by adsorption which uses the couple zeolite and water. Thus, through a mathematical model, we wrote the equations of balance at each part of the refrigerator and developed a program written in Fortran language in order to simulate the behavior of the refrigerator taking into account the climatic conditions of the city of Ouagadougou. The temperature changes of the glass, the absorbent plate, the condenser, the evaporator, the adsorbent bed and its pressure and the adsorbed mass were discussed.

The key findings are:

- For March and December, the average solar flux densities are 590 W/m^2 and 514 W/m^2 respectively. The amount of cold produced during these months is 6.391 MJ for the month of March and 4.642 MJ for the month of December. This gives a SCOP of 0.25 and 0.21 for the months of March and December.

- With an average daily solar flux density of 436 W/m^2 and 480 W/m^2 respectively for the months of August and October, the SCOP reached by our solar refrigeration system is 0.11 and 0.15, with a total product amount of 2.12 and 3.1 MJ.

The dynamic model thus developed allows to predict the real operation of the solar adsorption refrigerator and to evaluate its performance according to the climatic conditions of the city of Ouagadougou (Burkina Faso) for the hottest months and the coldest months of the year. The results obtained are very encouraging to continue to improve the performance of the solar adsorption refrigerator in order to use it in industrial and domestic domains.

Acknowledgements

References

[1] Anyanwu, E. (2000) Environmental Pollution: Restructuring the Refrigeration Industry as a Way out. *Environment Protection Engineering*, **26**, 17-28.

[2] Hadj Ammara, M., Benhaoua, B. and Balghouthi, M. (2015) Simulation of Tubular Adsorber for Adsorption Refrigeration System Powered by Solar Energy in Sub-Sahara Region of Algeria. *Energy Conversion and Management*, **106**, 31-40.
https://doi.org/10.1016/j.enconman.2015.09.013

[3] Umair, M., Akisawa, A. and Ueda, Y. (2014) Performance Evaluation of a Solar Adsorption Refrigeration System with a Wing Type Compound Parabolic Concentrator. *Energies*, **7**, 1448-1466. https://doi.org/10.3390/en7031448

[4] Qasem, N. and El-Shaarawi, M. (2013) Improving Ice Productivity and Performance for an Activated Carbon/Methanol Solar Adsorption Ice-Maker. *Solar Energy*, **98**, 523-542. https://doi.org/10.1016/j.solener.2013.10.018

[5] Chikouche, A. (2012) Using Solar Energy for Refrigeration Purposes in Algeria.

[6] Uyun, M.A., Miyazaki, T., Ueda, Y. and Akisawa, A. (2010) Performance Analysis of a Double-Effect Adsorption Refrigeration Cycle with a Silica Gel/Water Working Pair. *Energies*, **3**, 1704-1720. https://doi.org/10.3390/en3111704

[7] Hassan, H., Mohamad, A. and Al-Ansary, H. (2012) Development of a Continuously Operating Solar-Driven Adsorption Cooling System: Thermodynamic Analysis and Parametric Study. *Applied Thermal Engineering*, **48**, 332-341.
https://doi.org/10.1016/j.applthermaleng.2012.04.040

[8] Louajari, M., Mimet, A. and Ouammi, A. (2011) Study of the Effect of Finned Tube Adsorber on Theperformance of Solar Driven Adsorption Cooling Machine Using Activated Carbon-Ammonia Pair. *Applied Energy*, **88**, 690-698.
https://doi.org/10.1016/j.apenergy.2010.08.032

[9] Ousmane, M., Dianda, B., Kam, S., Konfe, A., Ky, T. and Bathiebo, D. (2015) Experimental Study in Natural Convection. *Global Journal of Pure and Applied Sciences*, **21**, 155-169. https://doi.org/10.4314/gjpas.v21i2.8

[10] Anyanwu, E. (2003) Review of Solid Adsorption Solar Refrigerator I: An Overview of the Refrigeration Cycle. *Energy Conversion and Management*, **44**, 301-312.
https://doi.org/10.1016/S0196-8904(02)00038-9

[11] Meunier, F. (2001) Adsorptive Cooling: A Clean Technology. *Clean Products and Processes*, **3**, 8-20. https://doi.org/10.1007/s100980000096

[12] Fadar, A.E. (2015) Thermal Behavior and Performance Assessment of a Solar Adsorption Cooling System with Finned Absorber. *Energy*, **83**, 674-684.
https://doi.org/10.1016/j.energy.2015.02.074

[13] Critoph, R.E. (1999) Adsorption Refrigerators and Heat Pumps. In: Burchell, T.D., Ed., *Carbon Materials for Advanced Technologies*, Elsevier, Amsterdam, 303-340.
https://doi.org/10.1016/B978-008042683-9/50012-1

[14] Mhimid, A., Jemni, A.A. and Nasrallah, B.S. (1997) Etude théorique des transferts couples de chaleur et de masse lors de la désorption du couple Zéolithe 13X-eau. *Revue Générale de Thermique*, **36**, 697-706.
https://doi.org/10.1016/S0035-3159(97)88434-6

[15] Jemni, A. and Ben Nasrallah, S. (1995) Study of Two-Dimensional Heat and Mass Transfer during Desorption in a Metal-Hydrogen Reactor. *International Journal of Hydrogen Energy*, **20**, 881-891. https://doi.org/10.1016/0360-3199(94)00115-G

[16] Critoph, R. and Turner, L. (1995) Heat Transfer in Granular Activated Carbon Beds in the Presence of Adsorbable Gases. *International Journal of Heat and Mass Transfer*, **38**, 1577-1585. https://doi.org/10.1016/0017-9310(94)00276-2

[17] Almers, A., Azzabakh, A. and Mimet, A. (2006) Optimal Design Study of Cylindrical Finned Reactor for Solar Adsorption Cooling Machine Working with Activated Carbon-Ammonia Pair. *Applied Thermal Engineering*, **26**, 1866-1875. https://doi.org/10.1016/j.applthermaleng.2006.01.021

[18] Chekirou, W., Boukheit, W. and Kerbache, T. (2007) Numerical Modeling of Combined Heat and Mass Transfer in a Tubular Adsorber of a Solid Adsorption Solar Refrigerator. *Revue des Energies Renouvelables*, **10**, 367-379.

[19] Hassan, H., Mohamad, A. and Bennacer, R. (2011) Simulation of an Adsorption Solar Cooling System. *Energy*, **36**, 530-537. https://doi.org/10.1016/j.energy.2010.10.011

[20] Mohamed, L., Abdelaziz, M. and Ahmed, O. (2011) Study of the Effect of Finned Tube Adsorber on the Performance of Solar Driven Adsorption Cooling Machine Using Activated Carbon-Ammonia Pair. *Applied Energy*, **88**, 690-698. https://doi.org/10.1016/j.apenergy.2010.08.032

[21] Naef, A., Qasem, M. and El-Shaarawi, A. (2013) Improving Ice Productivity and Performance for an Activated Carbon/Methanol Solar Adsorption Ice-Maker. *Solar Energy*, **98**, 523-542. https://doi.org/10.1016/j.solener.2013.10.018

[22] Li, M., Sun, C., Wang, R. and Cai, W. (2004) Development of No Valve Solar Ice Maker. *Applied Thermal Engineering*, **24**, 865-872. https://doi.org/10.1016/j.applthermaleng.2003.10.002

[23] Leite, A., Grilo, M., Andrade, R., Belo, F. and Meunier, F. (2007) Experimental Thermodynamic Cycles and Performance Analysis of a Solar-Powered Adsorptive Ice Maker in Hot Humid Climate. *Energy Renewable*, **32**, 697-712. https://doi.org/10.1016/j.renene.2006.03.002

[24] Muhammad, U., Atsushi, A. and Yuki, U. (2014) Performance Evaluation of a Solar Adsorption Refrigeration System with a Wing Type Compound Parabolic Concentrator. *Energies*, **7**, 1448-1466. https://doi.org/10.3390/en7031448

[25] Bakkas, M., Mada, M. and Tahri, M. (2001) Modélisation et Simulation du Transfert de Chaleur et de Masse à l'Intérieur d'un Réacteur de Charbon Actif Réagissant avec de l'Ammoniac Couplé à un Caloduc Annulaire à Eau. *Revue des Energies Renouvelables*, 19-24.

[26] Allouhi, A., Kousksou, T., Jamil, A., El Rhafiki, T., Mourad, Y. and Zeraouli, Y. (2015) Optimal Working Pairs for Solar Adsorption Cooling Applications. *Energy*, **79**, 235-247. https://doi.org/10.1016/j.energy.2014.11.010

[27] Leite, A.D.M. (2000) Performance of a New Solid Adsorption Ice Maker with Solar Energy Regeneration. *Energy Conversion and Management*, **41**, 1625-1647. https://doi.org/10.1016/S0196-8904(00)00011-X

[28] Guilleminot, J.M.F. (1987) Heat and Mass Transfer in a Non Isothermal Fixed Bed Solid Adsorbent Reactor a Uniform Pressure-Non Uniform Temperature. *International Journal of Heat and Mass Transfer*, **30**, 1595-1606. https://doi.org/10.1016/0017-9310(87)90304-8

[29] Mimet, A. (1991) Etude théorique et expérimentale d'une machine frigorifique à adsorption d'ammoniac sur charbon actif. Thèse de Doctorat, FPMs, Mons.

[30] Iloeje, O., Ndili, A. and Enibe, S. (1995) Computer Simulation of a $CaCl_2$, Solid Adsorption Solar Refrigerator. *Energy*, **20**, 1141-1151. https://doi.org/10.1016/0360-5442(95)00050-Q

[31] Eun, T.-H., *et al.* (2000) Enhancement of Heat and Mass Transfer in Silica-Expanded Graphite Coposite Blocks for Adsorption Heat Pumps: Part I. Characterisation of the Composite Blocks. *International Journal of Refrigeration*, **23**, 64-73. https://doi.org/10.1016/S0140-7007(99)00035-3

[32] Lemmini, F. and Errougani, A. (2007) Experimentation of a Solar Adsorption Refrigerator in Morocco. *Renewable Energy*, **32**, 2629-2641. https://doi.org/10.1016/j.renene.2007.01.004

[33] Pons, M., Laurent, D. and Meunier, F. (1996) Experimental Temperature Fronts For Adsorptive Heat Pump Applications. *Applied Thermal Engineering*, **16**, 395-404. https://doi.org/10.1016/1359-4311(95)00025-9

[34] Rahman, A., Miyazaki, T., Ueda, Y., Saha, B. and Akisawa, A. (2013) Performance Comparison of Three-Bed Adsorption Cooling System with Optimal Cycle Time Setting. *Heat Transfer Engineering*, **34**, 938-947. https://doi.org/10.1080/01457632.2012.753571

[35] Uyun, A., Akisawa, A., Miyazaki, T., Ueda, Y. and Kashiwagi, T. (2009) Numerical Analysis of an Advanced Three-Bed Mass Recovery Adsorption Refrigeration Cycle. *Applied Thermal Engineering*, **29**, 2876-2884. https://doi.org/10.1016/j.applthermaleng.2009.02.008

[36] Muhammad, U., Atsushi, A. and Yuki, U. (2014) Simulation Study of Continuous Solar Adsorption Refrigeration System Driven by Compound Parabolic Concentrator. *Renewable Energy Journal*, **7**, 1-12. https://doi.org/10.2174/1876387101407010001

[37] Lemmini, F., Buret-Bahraoui, J., Pons, M. and Meunier, F. (1992) Simulation des performances d'un réfrigérateur solaire à adsorption: 1. Comparaison des performances pour deux types de charbon actif. *International Journal of Refrigeration*, **15**, 159-167. https://doi.org/10.1016/0140-7007(92)90006-G

[38] Boubakri, A., Guilleminot, J. and Meunier, F. (2000) Adsorptive Solar Powered Ice Maker: Experiments and Model. *Solar Energy*, **69**, 249-263. https://doi.org/10.1016/S0038-092X(00)00063-3

[39] Kreussler, S. and Bolz, D. (2000) Experiments on Solar Adsorption Refrigeration Using Zeolite and Water. Laboratory for Solar Energy, University of Applied Sciences, Lubeck.

[40] Li, M., Wang, R., Xu, Y., Wu, J. and Dieng, A. (2002) Experimental Study on Dynamic Performance Analysis of a Flat-Plate Solar Solid-Adsorption Refrigeration for Ice Maker. *Renewable Energy*, **27**, 211-221. https://doi.org/10.1016/S0960-1481(01)00188-4

[41] Allouhi, A., Kousksou, T., Jamil, A. and Zeraouli, Y. (2014) Modeling of a Thermal Adsorber Powered by Solar Energy for Refrigeration Applications. *Energy*, **75**, 589-596. https://doi.org/10.1016/j.energy.2014.08.022

[42] Ouedraogo, E., Coulibaly, O. and Ouedraogo, A. (2012) Elaboration d'une année météorologique type de la ville de Ouagadougou pour l'étude des performances énergétiques des bâtiments. *Revue des Energies Renouvelables*, **15**, 77-90.

Nomenclature

Cp	Spécific heat (J/kg.K)	ΔH	Heat of adsorption/desorption (J/kg)
D	Constant in the Dubinin-Astakhov Equation	**Subscripts**	
Gn	Solar radiation (W/m²)	a	adsorption
m	mass (kg)	ads	adsorbent
n	Constant in the Dubinin-Astakhov Equation	d	desorption
P	Pressure (Pa)	cd	condenser
P_s	Saturation Pressure (Pa)	ev	evaporater
Q_f	Cold production (J)	v	glass
q	Water concentration inside the zéolithe (kg/kg)	ext	outside
S	Area (m²)	amb	ambient
T	Température (K)	zeo	zeolithe
t	Time (s)	min/max	minimum
W_o	Parameter of Dubinin-Astrakhov Equation (m³/kg)	max	maximum
L(T)	Latent heat of vaporization (J/kg)	g	generation
	Greek Letters:	cv	convection
α	absorptance	moy	average
τ	Transmitance	eau	water
Δt	Time step (s)		